FACTA UNIVERSITATIS
Ser: **Elec. Energ.** Vol. 25, N° 1, April 2012, pp. 1 - 14
DOI: 10.2298/FUEE1201001A

FIELD EMISSION – BASED MANY-VALUED PROCESSING USING CARBON NANOTUBE CONTROLLED SWITCHES, PART 1: FUNDAMENTALS

Anas N. Al-Rabadi[1], Marwan S. Mousa[2]

[1]Computer Engineering Department, The University of Jordan, Amman, Jordan
[2]Physics Department, Mu'tah University, Al-Karak, Jordan

Abstract. *In this first part of the article, basics of field emission will be presented which will be utilized within the second part of the article for the architecture effectuation of new Carbon Nanotube (CNT) – based controlled nano switches. To implement the field emission CNT – based controlled switch, four field emission CNTs that have single carbon nanotubes as the emitters were tested; two with single-walled CNT and two with multi-walled CNT. A tube with a tungsten tip was also used for comparison. The Fowler-Nordheim analysis of the DC current-voltage data provided reasonable values for the sizes and local fields of emitters. It is also shown within the new implementation of the controlled switch that square-wave pulses from a single laser diode with 20 mW power and 658 nm wavelength which is focused on each emitter increased the emitted current by 5.2% with the CNT and 0.19% with the compared tungsten tip.*

Key words: *carbon nanotubes, controlled switching, fowler-nordheim analysis, field emission, nanotechnology*

1. INTRODUCTION

The field of nanotechnology is a new interdisciplinary field of research that cuts across several fields of electronics, chemistry, physics and biology, which analyzes and synthesizes systems in the nano scale (10^{-9} m) such as nanoparticles, nanowires and carbon nanotubes (CNTs) [4,7,8,14,15,17,29,30,33,35,44]. The CNT technology is one of the several cutting-edge emerging technologies within nanotechnology, showing high efficiency and very wide range of applications in several various fields in science and technology [3-7,9,12,14,15,17,24,28,30,35,36,41,44]. Recent examples of such applications include: (1) TVs based on field-emission of CNTs that consume much less power, are thinner and have a much higher resolution than the best plasma-based TVs available, and (2) nanocircuits based on CNTs such as CNT Field Effect Transistors (FETs) that show big potentials for consuming less power and are much faster than the available silicon-based FETs.

Received October 12, 2011
Corresponding author: Anas N. Al-Rabadi
Computer Engineering Department, The University of Jordan, Amman, Jordan • E-mail: a.alrabadi@ju.edu.jo

Recently conducted simulations and experiments have shown that photomixing (i.e., optical heterodyning) in laser-assisted field emission could be used as a new microwave or terahertz (THz) source with a multi-octave bandwidth [1,11,13,23-26,29,31,34,37,38]. The field emitter tip used is much smaller than the wavelength of the incident optical radiation so quasi-static conditions require that the electric field of the radiation is superimposed on the applied static field to modulate the height of the energy barrier. Electrons tunnel from the tip into vacuum with a delay τ of less than 2 fs. Therefore, because the current-voltage characteristics of field emission are extremely nonlinear, it is shown that if two lasers are focused on the tip, the mixer current follows each cycle of the difference frequency of the two lasers from DC up to 500 THz (which is equal to $1/\tau$). It is also shown that the tip will withstand the applied static fields which are as high as 9 V/nm, so that incident laser radiation with comparable field strengths could produce a bright source of microwave or THz radiation.

Carbon nanotubes are excellent field emitters [9,10,13,16,19,29,36,38,39,41] and facilitate the miniaturization of electronic devices [3,4,6-9,15,17,24,26-28,30,33,35,36,41]. Furthermore, the kinetic inductance of CNT causes them to be high impedance (approximately 5 kΩ) transmission lines [28], and has shown that this effect can be used for the efficient broadband matching to the high impedance that is inherent in field emission. The static and dynamic characterizations of field emitters which consist of a single CNT, both single-walled (SWCNT) and multi-walled (MWCNT) were described [29] and the comparison to a field emitter consisting of an etched single crystal of tungsten was also performed.

This paper introduces a novel CNT field emission – based device that implements one fundamental building block in logic synthesis – the controlled switch [2,32,43], and the use of the new device in many-valued computations is also shown for the important case of ternary Galois logic (GF_3). Fig. 1 illustrates the layout of the introduced CNT-based system design methodology. Layer 1 shows the underlying utilized Galois field algebra. Layer 2 illustrates the field emission physics used in the operation of the new device. Layer 3 shows the technology of carbon nanotubes which is used in the synthesis of the new field emission – based device, and layers 4 - 6 show the hierarchical implementation of applications into the system level.

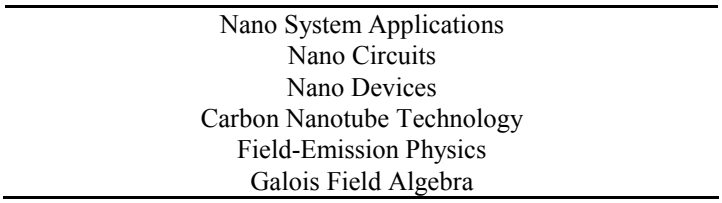

Fig. 1. The introduced and utilized CNT-based implementation hierarchy.

Basic background on CNT is presented in Section 2. The description and static characterization of the CNT-based field emitters along with the required experimental measurements that characterize the time-dependent response of field emission by single carbon nanotubes are presented in Section 3. Conclusions are presented in Section 4.

2. CARBON NANOTUBES

Carbon nanotubes have attracted attention in recent years not only for their relatively small dimensions and unique morphologies, but also for their potential implementations in many current and emerging technologies [3-9,12,14,15,17,24,28-30,33,35,36,41,44]. The CNT is made from graphite [8,14,15,17,30,33]. It has been observed that graphite can be formed in nano-scale in three forms: (1) Carbon Nanoball (CNB) (or buckyball) – a molecule consisting of 60 carbon atoms (C_{60}) that are arranged in the form of a soccer ball; (2) Carbon Nanotube (CNT) – a narrow strip of tiny sheet of graphite that comes mainly in two types: (a) multi-wall CNT (MWCNT) where each CNT contains several hollow cylinders of carbon atoms nested inside each other, and (b) single-wall CNT (SWCNT) that is made of a single layer of carbon atoms; and (3) Carbon Nanocoil (CNC) [8,14,15,17,30,33].

The CNT, which is a cylindrical sheet of graphite, is formed geometrically in two distinct forms which affect the corresponding CNT properties: (1) straight CNT in which a CNT is formed as a straight cut from a graphite sheet and rolled into a carbon nanotube, and (2) twisted CNT in which a CNT is formed as a cut at an angle from a graphite sheet and rolled into a carbon nanotube. Fig. 2 shows a typical carbon nanoball (i.e., buckyball), SWCNT, and Scanning Electron Microscopy (SEM) image of chemical vapor deposition (CVD) grown array of MWCNT towers.

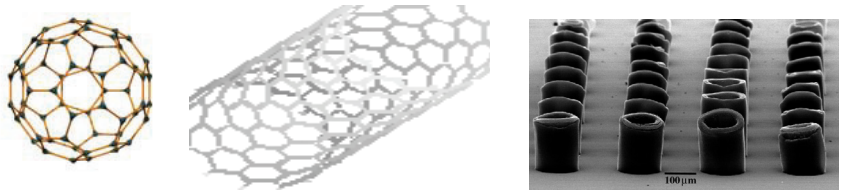

(a) (b) (c)

Fig. 2. Various formations and shapes of CNTs: (a) carbon nanoball (i.e., buckyball), (b) single-wall CNT, and (c) an image from the Scanning Electron Microscopy (SEM) of chemical vapor deposition (CVD) grown array of multi-walled CNT towers.

The newly emerging CNT technology has been implemented in many new promising applications [3-9,12,14,15,17,24,28-30,33,35,36,41,44]. This includes (1) TVs that are based on the field emission of CNTs that consume much less power, are thinner, and have a much higher resolution than the best plasma-based TVs available, (2) nano circuits based on CNTs such as CNT-based FETs that consume less power and are much faster than the available silicon-based FETs, (3) Carbon nanocoils that can be used as inductors in nanofilters and as nanosprings in nano dynamic systems, and (4) CNT rings. The CNT has also potential exciting applications such as (1) CNT probes, (2) new composite materials, (3) CNT data storage devices capable of storing 10^{15} bytes/cm^2, (4) drug delivery systems, (5) nano lithography, and (6) CNT gears in which larger gears drive smaller gears or vice versa. Fig. 3 shows an important example of a CNT application in electronic systems as a channel in a field effect transistor.

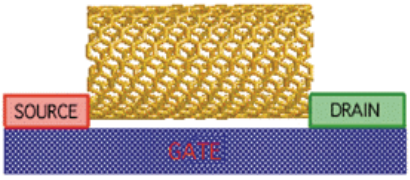

Fig. 3. The use of the CNT as a channel in FET devices.

The CNT growth, as observed using (1) Transmission Electron Microscopy (TEM), (2) Atomic Force Microscopy (AFM) and (3) Scanning Electron Microscopy (SEM), requires processes with correct conditions and materials. Currently, several methods for growing various types of CNTs exist [8,14,15,17,30,33]. This includes: (1) a big spark between two graphite rods, few millimeters apart, which are wired to a power supply in which a 10^2 Ampere spark between the two rods vaporizes carbon into hot plasma which partially re-condenses into the form of a CNT, (2) chemical vapor deposition (CVD) of a hot gas such as methane in which a substrate is placed in an oven, then the oven is heated to approximately 600 degrees Celsius and slowly methane is added; as methane decomposes, it frees carbon atoms that partially re-compose into the form of 0.6-1.2 nm in diameter SWCNTs, and (3) a laser blast of a graphite target in which laser pulses blast a graphite rod which generates hot carbon gas from which CNT forms.

Although the CNT has been grown into several forms, CNT use is still limited as compared to other wide spread technologies. This is mainly due to the fact that (1) it is still difficult to control exactly CNT growth into desired forms and (2) CNT growth is still very expensive due to the low yield of CNTs that meet the desired geometrical specifications (cf. the cost property in Table 1). The existing and rapidly growing wide usability of CNTs in several applications is due to the unique structural properties they possess. Table 1 summarizes most of these properties as compared to traditional counterparts [4].

For example, the field emission property is used in the recently developed highly efficient CNT-based TV and is used in newly developed prototype vacuum tube lamps in six colors that are twice as bright as conventional light bulbs, longer-lived and at least ten times more energy-efficient. The properties of current carrying capacity, thermal stability, power consumption and electron scattering qualify the CNT for very promising future use in highly efficient power transmission. The property of preserving the electron spin will be utilized in using the CNT for reliable quantum-based computations. The size property is very useful for using CNTs as nanowires that would result in decreasing the total size of areas and volumes that are occupied by wires and interconnects in the corresponding integrated circuits. The property of resilience is useful in building circuits and structures that have to maintain stress without structural damages. The CNT property of energy band gaps qualifies CNTs to be used in wide applications that require wide range of energy band gaps from the conductor state to the semiconductor state.

3. Carbon Nanotube - Based Field Emitters

This section presents important functional modeling of field emitters and the corresponding experimental setups and measurements that characterize the time-dependent

response of CNT-based field emission from which the operation of the new CNT field emission – based device will be demonstrated in the second part of this paper.

Table 1. Carbon nanotube properties.

Property	Single-Walled CNT	By Comparison
Size	0.6 - 1.8 nm in diameter	Electron beam lithography can create lines 50 nm wide and a few nm thick
Density	1.33 – 1.40 g/cm^3	Aluminum has a density of 2.7 g/cm^3
Tensile Strength	≈ 45·10^9 Pascals	High-strength steel alloys break at ≈ 2·10^9 Pascals
Resilience	Can be bent at large angles and re-straightened without damage	Metals and carbon fibers fracture at grain boundaries
Current Carrying Capacity	≈ 1·10^9 A/cm^2	Copper wires burn out at ≈ 1·10^6 A/cm^2
Field Emission	Can activate phosphors at 1 – 3 V if electrodes are spaced 1 micron apart	Molybdenum tips require ≈ 50 – 100 V/micrometer with very limited lifetimes
Heat Transmission	≈ 6,000 W/m·K at room temperature	Nearly pure diamond transmits ≈ 3,320 W/m·K
Temperature / Thermal Stability	Stable up to 2,800 C in vacuum and 750 C in air	Metal wires in microchips melt at ≈ 600 – 1,000 C
Cost	≈ 1,500 $/g	Gold sells for ≈ 40 $/g
Preservation of the Quantum Property of Electron Spin	Optimal; Very high	Low in regular conductors
Power Consumption	Very low	Higher in metal wires
Speed	Very high ≥ 1·10^{12} Hertz nanoscale switch	≥ 1,000 times as fast as processors available today
Electron Scattering (Resistance)	Almost none	Comparatively high
Energy Band Gaps	Easily tunable; Depends on CNT diameter and thus wide range of band gaps can be obtained: ≈ 0 (like a metal), as high as band gap of Silicon, and almost anywhere in between	No other known material can be so easily tuned

3.1. Description and static characterization of the field emitters

In order to perform the static modeling of CNT field emitters, four field emission carbon nanotubes, which are shown in Figs. 4(b)-4(e), were manufactured by Xintek, Inc. The

copper anode is at the right and the CNT emitter is mounted on a tungsten wire attached to the copper cylinder at the left as shown in Fig. 4(a). Figs. 4(b)-4(e) show the images of CNT emitters for each carbon nanotube [29] taken with a JEOL Ltd. model JEM 6300 SEM.

Carbon nanotubes M-1 and M-4 have a single MWCNT as the emitter, and carbon nanotubes C-3 and C-6 have a single SWCNT as the emitter. The used CNTs were formed in bundles that have diameters of 10-30 nm, but in each carbon nanotube the field emission is from the CNT at the end of the bundle where the electric field is most intense.

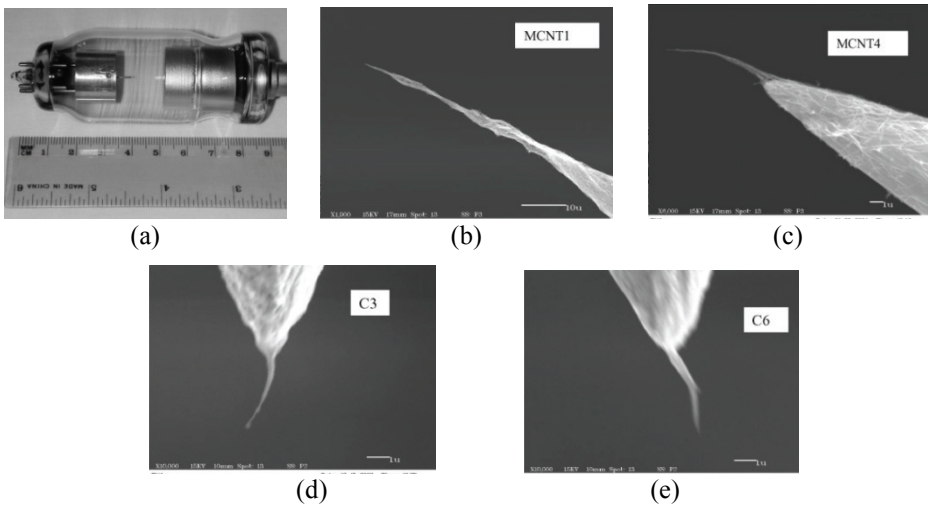

Fig. 4. Carbon nanotube – based field emission: (a) appearance of the field emission carbon nanotubes manufactured by Xintek, Inc. and (b) - (e) the Scanning Electron Microscopy (SEM) images of the CNT emitters in the four utilized carbon nanotubes. In the conducted imaging, the dimensions of the individual CNTs were not determined.

The DC current-voltage characteristics were measured for these four carbon nanotubes, as well as a field emitter tube from Leybold Didactic GmbH, which has an etched single crystal of tungsten as the emitter. All of the measurements that were made with the five tubes were performed at room temperature. The tungsten tip is mounted on a filament so that this tip is heated for cleaning shortly before each session of measurements. However, it is not possible to clean the CNT, which probably causes the "switch-on" effect in which the supply voltage must be momentarily increased well beyond the operating point to initiate field emission with the CNT.

The data from the DC measurements were reduced by the Fowler-Nordheim analysis [18,40] which is based on the following simplified form of the Fowler-Nordheim equation that provides the magnitude of the current density as a function of the applied static field for the field emission from a specific material [18,20,40]:

$$J = A\, E^2\, e^{(-B/E)} \tag{1}$$

where J and E are the magnitudes of the current density and the electric field intensity, $A = 1.541 \times 10^{-6}/\Phi$, and $B = 6.831 \times 10^{9}\, \Phi^{3/2}$. The work function $\Phi = 4.5$ eV for tungsten,

and for the CNT was set to $\Phi = 4.9$ eV for graphene. In order to apply the Fowler-Nordheim equation to the DC current-voltage data, the following equation was also used which is valid for a given carbon nanotube, where I is the field emission current and V is the potential applied between the anode and the cathode:

$$I = CV^2 e^{(-D/V)} \tag{2}$$

Equations (1) and (2) can be combined to obtain the following equations for the parameters S and R, which are used to characterize the field emitters:

$$S = CD^2/AB^2 \tag{3}$$

$$R \equiv V/E = D/B \tag{4}$$

where the parameter S refers to the effective emitting area which would be the physical area of the emitter if the current density were uniform over a fixed area and zero elsewhere, and the parameter R refers to the effective radius of curvature of the emitter and includes the effects of local intensification of the electric field caused by elongation of the emitter or the reduction of the field which may be caused by shielding due to adjacent structures.

The Fowler-Nordheim plots of the DC current-voltage data were conducted using $\ln(I/V^2)$ as the ordinate and (1/V) as the abscissa. Equation (2) requires that these plots should be straight lines and typically with correlation $c \approx -0.998$. Linear regressions based on these Fowler-Nordheim plots typically have a standard variance $\sigma \approx 0.08$, and the probability for the null-hypothesis, that no linear relationship exists, is less than 0.0001. The values of the parameters {C, D, S, R} were determined from the linear regressions. A series ballast resistor of 100 MΩ was typically used in the measurements. However, when the series ballast resistor was increased to 2.575 GΩ with carbon nanotube C-6, the obtained data were not consistent with the Fowler-Nordheim equation ($c = -0.846$, $\sigma = 0.738$) even though the emitted current was stable at each value of the applied static potential. Fig. 5 shows the anomalous data which were obtained using the 2.575 GΩ ballast resistor. In order to explain this effect, it is hypothesized that for currents greater than 500 nA, field emission with a single CNT may be intermittent, fluctuating at a high frequency. Thus, the average current, as measured by the DC microammeter, can be much greater with a large ballast resistor. This is because when the current is momentarily low, the voltage drop across the ballast resistor is at minimum so that high voltage occurs across the CNT, and this voltage causes a short-duration surge in the current.

Several other conducted experiments have also observed the instabilities in the field emission from a single CNT [9,10,16]. However, the performed works did not describe the bias circuits which were used so it is not possible to determine if these instabilities were exacerbated by increasing the ballast resistor. The data which are consistent with the Fowler-Nordheim equation were obtained with carbon nanotube C-6 when the ballast resistor was decreased to values including 100 MΩ or 595 MΩ.

The values of parameter R, the effective radius of curvature of the emitter, were found to vary within 77-110 nm for the four carbon nanotubes with CNT emitters. This suggests that values of the local electric field at the emitting sites were as high as 14 V/nm in some of these measurements. Others studying the field emission from various CNTs have provided approximate values for the electric field by dividing the applied voltage by the distance between the anode and the emitting tip, noting that this field would be intensified by the shape of the CNT, but not estimating the local electric field at the emitting sites [41].

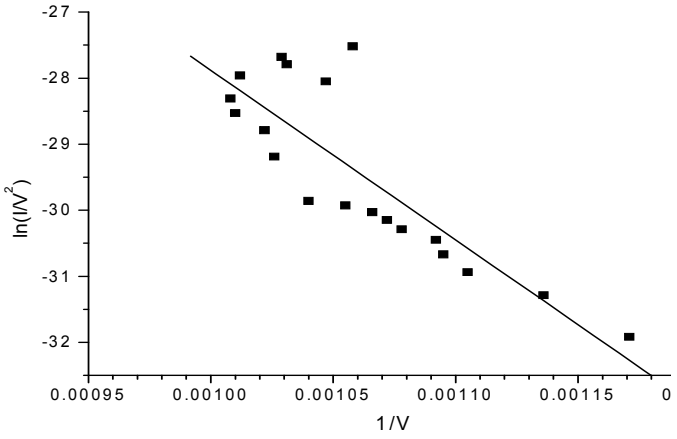

Fig. 5. The obtained Fowler-Nordheim plot for CNT C-6 with 2.575 GΩ ballast resistor.

The Fowler-Nordheim analysis gave a value of 91 nm for the effective radius of curvature of the emitter in the Leybold tube, suggesting that the local electric field was as high as 5 V/nm in some of the performed measurements [29]. Current densities as high as 10^9 and 10^{12} A/m^2 may be drawn from a tungsten emitter in steady-state and pulsed operation, respectively, and the corresponding values of the applied static field are 4.7 and 8.6 V/nm which may be considered as limiting field strengths for tungsten under these conditions. Thus, the value of the parameter R which was obtained for the Leybold tube appears to be reasonable.

The Fowler-Nordheim analysis also showed that the parameter S, the effective emitting area, varied within 81-230 nm^2 for the four carbon nanotubes with CNT emitters. If the current density was uniform, this would correspond to circular emitting spots having radii of approximately 5-9 nm. Others have used Lorenz microscopy to directly observe the emitting sites for field emission from MWCNT, and they found one or more sites having radii of several nm [19], and their data were in reasonable agreement with other performed experiments. The Fowler-Nordheim analysis also showed that the effective emitting area for the tungsten tip in the Leybold tube would correspond to a hemisphere with a radius of 290 nm. This result and the value of 91 nm for the effective radius of curvature of the emitter in the Leybold tube were in reasonable agreement with the radius of 100-200 nm which was specified by Leybold.

3.2. Experimental measurements of mixing at audio frequencies

Rigorous quantum simulations of laser-assisted field emission were performed which showed that the radiation from two lasers increases the DC current (optical rectification) and also causes harmonics and mixing terms with frequencies ($n_1f_1 + n_2f_2$), where f_1 and f_2 are the frequencies of the lasers and the integers n_1 and n_2 may be positive, zero or negative. However, the high-frequency terms are not seen in measurements of the current that passes through a field emission tube because the tube itself acts as a low-pass filter [27]. Antennas and transmission lines on field emitters have been made to couple microwave output power at the difference frequency ($f_1 - f_2$) [1,26], but these techniques were not implemented in the utilized tubes shown

in Fig. 4. Instead, the spectrum of the field emission current was determined when transformers were used to superimpose low-frequency voltages on the applied static field with f_1 = 1.67 kHz and f_2 = 1.10 kHz. These frequencies were chosen [27] because they are low enough that the effects of the capacitances and inductances within the tubes may be neglected.

To assist in the understanding of these phenomena, closed-form equations for the components of the field emission current may be obtained by using time-dependent perturbation with the Fowler-Nordheim equation. This method requires the adiabatic approximation that the frequencies of the oscillatory fields are low enough that the effects of the photon energy may be neglected [26]. Thus, the closed-form equations can be determined for all of the components of the current which are found in the rigorous quantum simulations [25]. However, with laser radiation it is necessary to multiply each term by the gain that is caused by a resonance in the interaction of the tunneling electrons and the radiation field [22,37-39].

For the two sinusoidal voltages that are superimposed on the applied static potential V_0 such that:

$$V = V_0 + V_1\cos(\omega_1 t) + V_2\cos(\omega_2 t) \tag{5}$$

then if V_1 and V_2 are much less than V_0 and the parameter D in Equation (2), and the frequencies $\{\omega_1, \omega_2\}$ are low enough that the effects of the photon energy may be neglected, then a 2nd order Taylor series expansion of Equation (2) about the operating point (V_0, I_0), where there is only the applied static potential V_0 and the DC current I_0, provides the following equation for the total current:

$$I = I_0 + I_\Delta + I_{F1} + I_{F2} + I_{H1} + I_{H2} + I_S + I_D \tag{6}$$

where the step increase of the DC current, the two fundamental terms, the two second harmonic terms, and the sum and difference terms are provided using the following equations, respectively:

$$I_\Delta = I_0(D^2/4V_0^2)[(V_1/V_0)^2+(V_2/V_0)^2][1+2V_0/D+2V_0^2/D^2 \tag{7a}$$

$$I_{F1} = I_0(D/V_0)(V_1/V_0)[1+2V_0/D]\cos(\omega_1 t) \tag{7b}$$

$$I_{F2} = I_0(D/V_0)(V_2/V_0)[1+2V_0/D]\cos(\omega_2 t) \tag{7c}$$

$$I_{H1} = I_0(D^2/4V_0^2)(V_1/V_0)^2[1+2V_0/D+2V_0^2/D^2]\cos(2\omega_1 t) \tag{7d}$$

$$I_{H2} = I_0(D^2/4V_0^2)(V_2/V_0)^2[1+2V_0/D+2V_0^2/D^2]\cos(2\omega_2 t) \tag{7e}$$

$$I_S = I_0(D^2/2V_0^2)(V_1/V_0)(V_2/V_0)[1+2V_0/D+2V_0^2/D^2]\cos[(\omega_1+\omega_2)t] \tag{7f}$$

$$I_D = I_0(D^2/2V_0^2)(V_1/V_0)(V_2/V_0)[1+2V_0/D+2V_0^2/D^2]\cos[(\omega_1-\omega_2)t] \tag{7g}$$

Transformers were used to couple the two floating battery-operated Wien bridge oscillators in series with the high-voltage anode circuit of each of the five field emission tubes in order to superimpose low-frequency sinusoidal signals on the applied static field. The oscillators provided the high voltages $V_1 = V_2 = 120$ V which are required to cause a measurable effect on the current. The full series loop of the electrical circuit included the high-voltage power supply, 100 MΩ ballast resistor, the secondary windings of the transformers for the oscillators, the field emission tube, a DC microammeter, and 1 MΩ resistor to ground which was a shunt for the digital oscilloscope.

The capacitive shunts were used to eliminate the effects of the high-voltage power supply, the ballast resistor, and the DC microammeter on the currents at the six frequencies. Thus, the DC equivalent circuit consists of the high-voltage power supply, a resistance of 101 MΩ, the tube modeled by the two current sources I_0 and I_Δ in parallel, and the DC microammeter. The equivalent circuit at each of the six frequencies consists of the tube modeled by the respective current source, in series with the parallel combination of the 1 MΩ resistor and the digital oscilloscope.

The used two oscillators were set to the frequencies f_1 = 1.67 kHz and f_2 = 1.10 kHz, and the step increase in the DC current as well as the components of the current at the six frequencies $\{f_1, f_2, 2f_1, 2f_2, (f_1 + f_2), (f_1 - f_2)\}$ were determined. These frequencies correspond to {1.67, 1.10, 3.34, 2.20, 2.77, 0.57} kHz, respectively. Each of the measured currents were compared with the values calculated using the respective equivalent circuit with Equations (7a – 7g).

In comparison with the Leybold tube, it was found that the currents at the fundamental frequencies f_1 and f_2 were each within 5% of the predicted values, and the step increase in the DC current and the currents at each of the other four frequencies were each within 10% of the predicted values. The measured increase in the DC current and the currents at the six frequencies, were each between 1 and 2 times the predicted values for carbon nanotubes M-4 and C-6, and between 3 and 4 times the predicted values for carbon nanotube M-1. In the conducted measurements, carbon nanotube C-3 was very unstable to permit measuring any of the currents at the six frequencies. As it was noted earlier, it was not possible to clean the CNT, and this caused the values of the parameter D in Equations (7a – 7g) to be less reproducible for the CNT than it is for the Leybold tube, where the greater errors in the measurements with the CNT are attributed to this effect.

3.3. Experimental measurements of the variation in the DC current caused by a laser source

While there are no means to couple microwave or terahertz power from any of the used five tubes, the step increase in the DC current that is caused by focusing a single square-wave modulated laser diode with the specifications of power = 20 mW and wavelength = 658 nm on the field emission tip. The laser diode was maximally-focused to provide a measured Gaussian profile with a power flux density of approximately 10^7 W/m^2 at the tip. Equations (7a) and (7g) show that this measured current step is equal to ½ of the peak value of the mixer current that would be generated if two stabilized tunable lasers each provided the same power flux density. Thus, this low-frequency measurement can be used to estimate the mixer current obtained by photomixing with these same field emitters.

The laser diode was amplitude-modulated with a square-wave envelope and the field emission current was measured with a digital oscilloscope shown in Fig. 6. It was observed earlier that field emission tube itself behaves like a low-pass filter [27]. Equation (7a) shows that the increase in the field emission current (I_Δ) acts as a current source, and it can be shown that when a square-wave current source is fed to a parallel R-C circuit, the voltage across the resistor has a saw-tooth waveform with a peak-to-peak value of:

$$V_{pp} = R\, I_\Delta\, (1 - e^{-1/2\tau f}) / (1 + e^{-1/2\tau f}) \qquad (8)$$

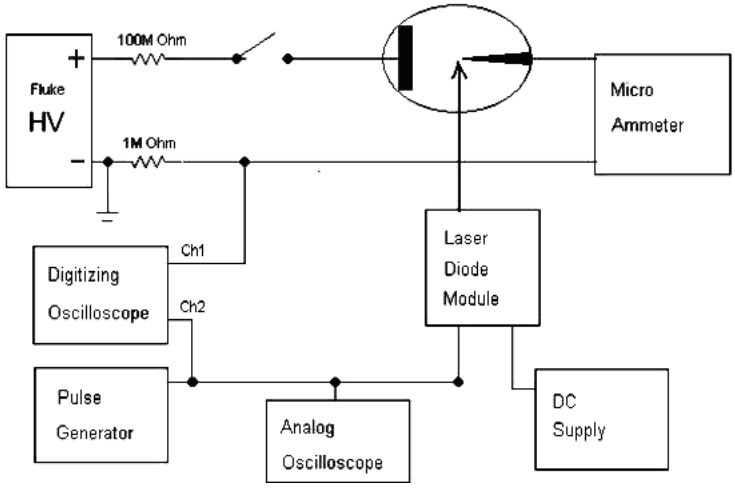

Fig. 6. The used experimental configuration for the conducted measurements with a square-wave modulated laser diode.

where I_Δ is the peak-to-peak value of the current waveform and $\tau = RC$. Equation (8) shows that $V_{pp0} \equiv V_{pp}(f = 0) = R\, I_\Delta$ and $V_{pp} = R\, I_\Delta/4\tau f = V_{pp0}/4\tau f$ for $f >> 1/\tau$.

The peak-to-peak value of the voltage across the resistor was measured as a function of the modulation frequency for each of the tubes. A DC current of 1 μA was used with each of the four used CNT tubes, and 8 μA was used with the Leybold tube. However, carbon nanotube C-6 could not be used in this experiment because ripples in the glass envelope interfered with focusing of the laser on the tip. Least-square regression was used to determine the values of I_Δ and τ from these data.

Fig. 7 shows the measured value of the apparent peak-to-peak amplitude of the field emission current as a function of the modulation frequency for carbon nanotube M-4, and Table 2 shows the parameters that were measured with calculated characteristics of the tubes. Clearly, Fig. 7 illustrates the inverse behavior which is predicted at frequencies that are much greater than $(1/\tau)$.

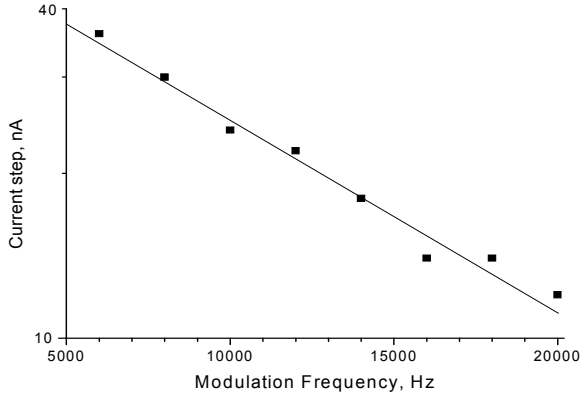

Fig. 7. The step in current caused by laser vs. modulation frequency for CNT M-4.

Table 2. Measured and calculated parameters for the step-increase in the DC current which is caused by a laser.

Tube	M-1	M-4	C-3	Leybold
DC current I_0, μA	1.0	1.0	1.0	8.0
DC voltage across tube, V	980	840	920	4600
R, kΩ	500	500	500	1000
T, μs	110	80	86	510
C, pF	220	160	170	510
I_Δ, pA	56	83	48	16
(I_Δ / I_0), %	5.6	8.3	4.8	0.20

From Table 2, one can observe that the actual value of I_Δ for carbon nanotube M-4 is 83 pA which is observed in the data that were taken for much lower modulation frequencies. Table 2 also shows that the mean increase in the DC current is 6.2 % for the three tubes with CNT, as compared with 0.20 % for the Leybold tube. This suggests that if two stabilized tunable lasers each provided the same power flux density, the peak value of the mixer current, occurring at the difference frequency $(f_1 - f_2)$, would be within an average of 12 % of the DC current for the tubes with CNT, as compared with 0.40 % for the Leybold tube.

4. CONCLUSIONS

Fundamentals of field emission are introduced in this first part of the article. For the realization of the new CNT field emission – based switching device, four field emission tubes having single CNT as the emitters were tested, and a tube having a tungsten tip was used for the corresponding comparison. The Fowler-Nordheim analysis of the DC current-voltage data gave reasonable values for the local fields at the emitters and the sizes of the emitter sites. Also, two audio-frequency oscillators superimposed sinusoidal signals on the applied static field, thus increasing the DC emitted current and causing components of the current at the two fundamental frequencies, the second harmonics and the sum and difference frequencies, which are in good agreement with the associated theory. A single square-wave modulated laser diode of power p = 20 mW and wavelength λ = 658 nm focused on each emitter, increased the emitted current by an average of 6.2 % during each laser pulse with the CNT and 0.20 % with the tungsten tip. Tubes were previously manufactured in which antennas and transmission lines couple the microwave power that is generated by photomixing in laser-assisted field emission to an external load, and these tubes have used emitters of tungsten (W) and molybdenum (Mo).

The measurements conducted with the CNT suggest that the mixer current could be 30 times greater if either SWCNT or MWCNT were used in place of the metal emitters, which would increase the microwave output power by 30 dB as a considerable improvement. While it was observed that, when the laser beam is turned on, then the field emission current increases with a characteristic time that is similar to the calculated thermal relaxation time of the field emitter (so this effect could be thermal), it was shown that the slow rise time for the current in such experiments is due to circuit effects. Also recently, electron pulses with durations of under 70 fs were generated by irradiating a field emitter

with a low-power femtosecond laser, where it has been shown that this effect is non-thermal; the operating parameters may cause either photofield emission or optical field emission to be dominant. More pertinently, laser radiation was utilized to increase the field emission current from a cathode with a dense field of CNT by a factor of 18, and was shown that this is not a thermal effect by comparing the corresponding data with the effect of elevated temperatures on the field emission from the used CNT.

A 2-to-1 controlled switch is a basic building block in "switch logic", where the concept of the *switch logic* is that logic circuits are implemented as combination of switches, rather than a combination of logic gates as in the *gate logic*, which proves to be less-costly in synthesizing a wide variety of logic circuits and systems. Since the controlled switch is of fundamental importance in logic design, the new device can have a wide spectrum of implementations in a wide variety of nano circuits and systems.

REFERENCES

[1] K. Alonso and M. J. Hagmann, "Comparison of three different methods for coupling of microwave and terahertz signals generated by resonant laser-assisted field emission," *Journal of Vacuum Science & Technology B*: *Microelec. Nanometer Structures*, 19(1): 68-71, 2001.

[2] A. N. Al-Rabadi, *Reversible Logic Synthesis*: *From Fundamentals to Quantum Computing*, Springer-Verlag, New York, 2004.

[3] A. N. Al-Rabadi, "Carbon nano tube (CNT) circuits," In Proceedings of the Post-Binary Ultra Large Scale Integration (ULSI) Workshop, Toronto, Canada: 2004, pp. 44-49.

[4] A. N. Al-Rabadi, "Carbon nano tube (CNT) multiplexers for multiple-valued computing," *Facta Universitatis – Electronics and Energetics*, vol. 20, no. 2, pp. 175 -186, 2007.

[5] A. N. Al-Rabadi, "New dimensions in non-classical neural computing, Part I: three-dimensionality, invertibility, and reversibility," *Int. J. Intell. Comp. Cyber.*, Emerald, vol. 2, no. 2, pp. 348-385, 2009.

[6] A. N. Al-Rabadi, "New dimensions in non-classical neural computing, Part II: quantum, nano, and optical," *Int. J. Intell. Comp. Cyber.*, Emerald, vol. 2, no. 3, pp. 513-573, 2009.

[7] A. N. Al-Rabadi, *Carbon NanoTube* (*CNT*) *Multiplexers, Circuits, and Actuators*, United States Patent and Trademark Office, Patent No. US 7,508,039 B2, U.S.A., 24 March 2009.

[8] G. Amaratunga, "Watching the nanotube," *IEEE Spectrum*, pp. 28-32, 2003.

[9] J.-M. Bonard, J.-P. Salvetat, T. Stöckli, L. Forro, and A. Chatelain, "Field emission from carbon nanotubes: perspectives for applications and clues to the emission mechanism," *Applied Physics A*: *Materials Science & Processing*, 69(3): 245-254, 1999.

[10] J.-M. Bonard, K. A. Dean, B. F. Coll, and C. Klinke, "Field emission of individual carbon nanotubes in the scanning electron microscope," *Phy. Rev. Let.*, 89(19): 197602-1:4, 2002.

[11] M. Brugat, M. S. Mousa, E. P. Sheshin, and M. J. Hagmann, "Measurement of field emission current variations caused by an amplitude modulated laser," *Mat. Sci. Eng. A*, 327(1): 7-15, 2002.

[12] P. J. Burke, "Luttinger liquid theory as a model of the gigahertz electrical properties of carbon nanotubes," *IEEE Transactions on Nanotechnology*, 1(3): 129-144, 2002.

[13] H.-F. Cheng, Y.-S. Hsieh, Y.-C. Chen, and I.-N. Lin, "Laser irradiation effect on electron field emission properties of carbon nanotubes," *Diam. and Related Mat.*, 13(4-8):1004-1007, 2004.

[14] P. G. Collins and P. Avouris, "Nanotubes for electronics," *Scientific American*, pp. 62-69, 2000.

[15] P. G. Collins, M. S. Arnold, and P. Avouris, "Engineering carbon nanotubes and nanotube circuits using electrical breakdown," *Science*, vol. 292, 2001.

[16] K. A. Dean and B. R. Chalamala, "Current saturation mechanisms in carbon nanotube field emitters," *Applied Physics Letters*, 76(3): 375-377, 2000.

[17] V. Derycke, R. Martel, J. Appenzeller, and P. Avouris, "Carbon nanotube inter- and intramolecular logic gates," *Nano Letters*, vol. 0, no. 0, A - D, 2001.

[18] R. H. Fowler and L. W. Nordheim, "Electron emission in intense electric fields," *Proc. Royal Society A*: *Mathematical, Physical and Engineering Sciences*, 119(781): 137-181, 1928.

[19] T. Fujieda, K. Hidaka, M. Hayashibara, T. Kamino, Y. Ose, H. Abe, T. Shimizu, and H. Tokumoto, "Direct observation of field emission sites in a single multiwalled carbon nanotube by Lorenz microscopy," *Japanese Journal of Applied Physics*, 44(4A): 1661-1664, 2005.

[20] R. Gomer, "Field emission and field ionization," *American Vacuum Society Classics*, American Institute of Physics (AIP), 1993.

[21] M. Haghparast and K. Navi, "Design of a novel fault tolerant reversible full adder for nanotechnology based systems", *World Applied Sciences J.*, vol. 3, no.1, pp. 114-118, 2008.

[22] M. J. Hagmann, "Mechanism for resonance in the interaction of tunneling particles with modulation quanta," *Journal of Applied Physics*, 78(1): 25-29, 1995.

[23] M. J. Hagmann, "Stable and efficient numerical method for solving the Schrödinger equation to determine the response of tunneling electrons to a laser pulse," *International Journal of Quantum Chemistry*, 70(4-5): 703-710, 1998.

[24] M. J. Hagmann, "Simulations of photon-assisted field emission: their significance in basic science and device applications," *Ultramicroscopy*, 79(1-4): 115-124, 1999.

[25] M. J. Hagmann, "Single-photon and multiphoton processes causing resonance in the transmission of electrons by a single potential barrier in a radiation field," *International Journal of Quantum Chemistry*, 75(4-5): 417-427, 1999.

[26] M. J. Hagmann, "Wide-band-tunable photomixers using resonant laser-assisted field emission," *Applied Physics Letters*, 83(1): 1-2, 2003.

[27] M. J. Hagmann, M. S. Mousa, M. Brugat, E. P. Sheshin, and A. S. Baturin, "Large-signal and small-signal electronic equivalent circuits for a field electron emitter," *Surface and Interface Analysis*, 36(5-6): 402-406, 2004.

[28] M. J. Hagmann, "Isolated carbon nanotubes as high-impedance transmission lines for microwave through terahertz frequencies," *IEEE Transactions on Nanotechnology*, 4(2): 289-296, 2005.

[29] M. J. Hagmann and M. S. Mousa, "Time-dependent response of field emission by single carbon nanotubes," *Jordan Journal of Physics*, vol. 1, no. 1, pp. 1-7, 2008.

[30] J. R. Heath and M. A. Ratner, "Molecular electronics," *Physics Today*, pp. 43-49, 2003.

[31] P. Hommelhoff, Y. Sortais, A. Aghajani-Talesh, and M. A. Kasevich, "Field emission tip as a nanometer source of free electron femtosecond pulses," *Phy. Rev. Let.*, 96(7): 077401-1:4, 2006.

[32] R. C. Jaeger, *Microelectronic Circuit Design*, McGraw-Hill, New York, 1997.

[33] J. Jiao, E. Einarsson, D. W. Tuggle, L. Love, J. Prado, and G. M. Coia, "High-yield synthesis of carbon coils on tungsten substrates and their behavior in the presence of an electric field," *Journal of Materials Research*, vol. 18, no. 11, pp. 2580-2587, 2003.

[34] M. J. G. Lee and E. S. Robins, "Thermal relaxation of a laser illuminated field emitter," *Journal of Applied Physics*, 65(4): 1699-1706, 1989.

[35] K. Likharev, "Hybrid semiconductor-molecular nanoelectronics," *Ind. Phy.*, pp. 20-23, 2003.

[36] Y. Liu and S. Fan, "Field emission properties of carbon nanotubes grown on silicon nanowire arrays," *Solid State Communications*, 133(2): 131-134, 2005.

[37] A. Mayer and J.-P. Vigneron, "Quantum-mechanical simulations of photon-stimulated field emission by transfer matrices and Green's functions," *Phy. Rev. B*, 62(23): 16138-16145, 2000.

[38] A. Mayer, N. M. Miskovsky, and P. H. Cutler, "Photon-stimulated field emission from semiconducting (10, 0) and metallic (5, 5) carbon nanotubes," *Phy. Rev. B*, 65(19): 195416-1:6, 2002.

[39] A. Mayer, N. M. Miskovsky, and P. H. Cutler, "Three-dimensional simulations of field emission through an oscillating barrier from a (10, 0) carbon nanotube," *Journal of Vacuum Science & Technology B*, 21(1): 395-399, 2003.

[40] L. W. Nordheim, "The effect of the image force on the emission and reflexion of electrons by metals," *Proc. Royal Society A*: *Math., Phy. Eng. Sciences*, 121(788): 626-639, 1928.

[41] A. N. Obraztsov, I. Pavlovsky, A. P. Volkov, E. D. Obraztsova, A. L. Chuvilin, and V. L. Kuznetsov, "Aligned carbon nanotube films for cold cathode applications," *Journal of Vacuum Science & Technology B*, 18(2): 1059-1063, 2000.

[42] B. Parhami, "Fault-tolerant reversible circuits," In Proc. 40th Asilomar Conf. Signals, Systems and Computers, Pacific Grove, CA: 2006, pp. 1726-1729.

[43] D. A. Patterson and J. L. Hennessy, *Computer Organization and Design*: *The Hardware / Software Interface*, Morgan-Kaufmann, 2008.

[44] R. Tarkiainen, M. Ahlskog, J. Penttila, L. Roschier, P. Hakonen, M. Paalanen, and E. Sonin, "Multiwalled carbon nanotube: Luttinger versus Fermi liquid," *Phy. Rev. B*, 64(19): 195412-1:4, 2001.